Polar Geophysical Institute

Kola Scientific Center

EISCAT UHF RADAR MEASUREMENTS AND NUMERICAL SIMULATION OF ELECTRON DENSITY VARIATIONS INDUCED BY HEATING OF THE D- AND E-REGIONS

Pashin A. B., Belova E. G. (Polar Geophysical Institute, Apatity, 184200, Russia), and Turunen E. (Sodankyla Geophysical Observatory, FIN-99600, Finland)

Apatity 1997

Abstract

A D-region incoherent scatter experiment was run on October 27, 1985, using the EISCAT UHF radar. During one hour the ionosphere was heated by a 5.4 MHz radio wave. The effective radiated power of 260 MW was repeatedly on for 230 seconds and off for 230 seconds. The incoherently backscattered power was interpreted as electron density, with correction for the enhanced electron temperature. The electron temperature was numerically estimated by solving the equations governing the electron energy balance and the radio wave passage through the ionosphere. Time variations of the deduced electron density are compared with the theoretically calculated variations. For this comparison the ionization-recombination balance equation was solved during heating. The deduced and theoretical electron densities show similar large scale time behavior, evidencing an overall increase of electron density due to artificial heating.

1. Introduction.

Absorption of powerful HF radio waves in the ionosphere leads to enhancement of electron temperature (Gurevich and Shvartsburg, 1973; Stubbe and Kopka, 1977). Electron temperature in the lower ionosphere may change by a factor of 5-8 (Tomko, 1980; Stubbe et al., 1982). When the modulation period of the artificial heating is of the order of some tens of seconds or more, variations in electron density are expected because the recombination rate depends on electron temperature. According to the numerical estimations carried out by Itkina and Krotova (1981); Pashin et al. (1995), the magnitude of the electron density variations may be 5-10 percent of the background value in the lower ionosphere .

Incoherent scatter observations of the F-region during ionospheric heating, using the EISCAT UHF radar, were reported by Jones et al. (1986). Enhancement of electron temperature was detected from the measured ion-line spectrum with a height resolution of 27 km. Heater induced electron density fluctuations in the F-region above Tromso, Norway have been derived for the first time from EISCAT backscattered power data by Honary et al. (1993). But as the authors note, it is often very difficult to obtain the magnitudes of the temperature and electron density variations with a reasonable accuracy, because the signal-to-noise ratio is too small. This problem was also noted by Schlegel et al. (1987).

In this paper we suggest to use the estimates of electron temperature from a numerical simulation that to derive the fluctuations of plasma density in the lower ionosphere during a heating experiment from the measured backscattered power data.

2. Description of the experiment

A special D-region EISCAT experiment (Turunen, 1986) with altitude coverage from 70 to 113 km and altitude resolution of 1.05 km was run on October 27, 1985 from 12.05 UT to 23.00 UT using the UHF 931.5 MHz radar. Originally, the data was recorded with a time resolution of 10 seconds but for later analysis different integration times of the order of 1-4 min were used. During one hour starting at 12.30 UT the ionosphere was heated with the Tromso Heating Facility. The transmitters operated at the frequency of 5.423 MHz in ordinary mode with a cycle of 230 s on and 230 s off, and an effective radiated power (ERP) of 260 MW.

The experiment was run during a geophysically quiet time. The sum of the three-hourly Kp indices for that day was 7+ and the daily average of the solar 10.7 cm radio flux was 78.5. The variations of ionization in the D- and E-regions were determined by the change of the solar zenith angle during sunset. Fig. 1 demonstrates the raw electron density measured by EISCAT at all observed altitudes versus time. The raw electron density is calculated from the backscattered power, neglecting the existence of negative ions and the finite Debye length effects at the lower D-region. Data is integrated for one minute in time and 6 km in altitude. The periods when the heater was turned on are marked. An effect of the heating pulse on the lower ionosphere is evident from Fig. 1. We can see an apparent decrease in the raw electron density estimate during the periods, when the heater is turned on. At the altitudes below 80 km the signal is so weak that the data appears noisy with the used time integration. On the other hand, above the altitude of 95 km the data is not applicable for a proper calibrated electron density estimate due to the design limitations of the used incoherent scatter experiment.

From the ion line component of the incoherent scatter spectrum, we can write an expression which relates the measured radar data with physical parameters:

$$N^{raw} = \frac{2N_e(1+\lambda)}{\left[1+\frac{T_e}{T_i}+\left(\frac{4\pi 69}{\lambda_r}\right)^2\frac{T_e}{N_e}\right]\left[1+\left(\frac{4\pi 69}{\lambda_r}\right)^2\frac{T_e}{N_e}\right]} \qquad (1)$$

where N^{raw} is the raw electron density estimate derived from backscattered power, N_e is the electron density, T_e and T_i are the electron and ion temperatures, respectively, λ is the negative ion to electron density ratio, and λ_r is the radar wavelength.

It is known that the characteristic time for the electron temperature change at the altitude of 100 km is of the order of a few tens of milliseconds (Mityakov et al., 1989), and

that electron density changes more slowly. Thus N^{raw} should reflect nearly momentary changes of electron temperature as well as slow (characteristic time of the order of some tens of seconds and more) variations of electron density after the heater is turned on. Thus at the moment of heater turning on, electron temperature increases and electron density has no enough time to change. According to expression (1) the value of N^{raw} decreases just after the heater is switched on. Then electron temperature is settled to be constant and electron density starts to increase. However, it changes very weakly within a heating impulse. It would be difficult to quantify these changes through the noise fluctuations in the original data with the time resolution of 10 seconds and the altitude resolution of 1.05 km. In order to see the temporal effects due to heating, the data of Fig. 1 is replotted in Fig.2 with the full time resolution of 10 seconds but integrated through the altitude range from 80 km to 95 km.

One can recognize a cubic equation for the actual electron density N_e in expression (1). Only one of the roots of this equation is a physical solution. The corrected electron density N_e at some altitude is determined by the measured value of the raw electron density N^{raw}, the electron to ion temperature ratio T_e / T_i and the negative ion to electron concentration ratio λ. We take λ to be equal to zero which is a reasonable assumption above 80 km in the sunlit ionosphere. The value of T_e we estimated from a numerical simulation.

3. Numerical modelling.

In order to calculate the electron temperature change due to ionospheric heating, we numerically solve the system of equations which describe the electron energy balance and the passage of a radio wave through the ionospheric plasma in the following form:

$$\frac{3}{2} k_B N_e \frac{\partial T_e}{\partial t} = Q - L \qquad (2)$$

$$\frac{\partial S}{\partial z} = -2kS = Q \qquad (3)$$

where Q is the electron energy absorption rate due to HF heating, L is the rate of electron energy losses due to collisions, k_B is the Boltsmann s constant, S is the power flux density of the heating radio wave and k is the absorption coefficient.

We calculate a steady-state value of the electron temperature, taking into account all significant electron collision processes for the determination of L. These can be described by introducing an effective collision frequency ν_{eff} as $L = \nu_{eff}\, \delta\, \Delta T_e$, where δ is the fraction of energy lost by the electron in one collision. We use expressions of L as given by Stubbe and Varnum (1972) and Prasad and Furman (1973). The method of solving this system of equations was reported in detail by Belova et al. (1995). The neutral temperature profile and neutral concentrations we took from the CIRA (1972) model.

The initial electron density profile is deduced from the backscattered power just before and after the heating experiment, assuming $T_e = T_i = T_n$, where T_n is the neutral temperature. Radar measurements supply us information about electron density only above the altitude of 70 km. Moreover the interpretation of backscattered power as electron density is affected by the existence of negative ions in the lower D-region and we have reliable estimates of electron density only above the altitude of 80 km. Thus there is some arbitrariness in our calculations in the lower D-region. The absolute magnitude of electron density in the altitude range from 60 km to 70 km is important in the calculation of the altitude profile of the enhanced electron temperature. Translucence and enhanced absorption effects on propagation of the heating radio wave may occur in the lower D-region (Belova et al., 1995). In our calculations we look over different trial electron density profiles at this height range. In Fig. 3 (top) we present a set of electron density profiles with different density values at the height interval from 60 to 78 km. As a result we obtain values of electron temperature in the height range from 60 to 150 km with an altitude step of 0.5 km. The calculated electron temperature profiles, corresponding to the electron density profiles of Fig. 3 (top) are shown in Fig. 3 (bottom). This figure demonstrates that electron density in the high interval from 60 to 78.5 km significantly affects on electron temperature profile during heating. Less electron density leads to the higher values of electron temperature disturbance in the lower ionosphere. The altitude of T_e maximum decreases with the electron density increase.

4. Electron density variations.

The temporal electron density variations in the lower ionosphere corresponding to electron temperature profiles of Fig. 3 (bottom), are shown in Fig. 4. They were calculated from the measured values of the raw Ne and the modelled values of electron

temperature, using expression (1). To avoid a significant scattering in electron density data we integrated them over the altitudes from 80 km to 95 km and used 230 seconds running averaging. The resulting variations have a different phase relative to heating impulse. Calculated variations are in phase with the heating impulses for the profile with poor initial electron density in the lower ionosphere. We believe that it is related with the overestimation of electron temperature enhancement after the heater was switching on. In contrary rather small values of disturbed electron temperature which should be for profile with maximum electron density leads to out of phase variations with the heating status plot. Note that this running averaging gives the start of electron density changes before heating impulse switching-on. We suppose that the profile of initial electron density which gives calculated variations of 90 degrees phase shifted relative the heater is the best for EISCAT measurements interpretation using the formula (1). In our case for 2nd, 3rd, and 4th pulses this is observed for the moderate profile. Before and during fifth pulse variations in all calculated curves are in-phase. It may be due to significant variations of ionization rate which we didn't take into account.

The moderate profile was taken for calculations of electron density profiles for 10 seconds EISCAT data. Integrated from 80 km to 95 km values are shown in Fig. 5. Significant scattering of electron density data is shown but we would like to put attention in this figure to the absent of the sharp variations similar to those of raw electron density (Fig.2).

Fig. 6 shows electron density derived from raw Ne and using 230 seconds running averaging (solid line). In this figure we also present a theoretically calculated electron density by dashed line. The electron number density N_e ignoring the plasma transport, is determined from:

$$\frac{\partial N_e}{\partial t} = q - \alpha_{eff} N_e^2 \qquad (4)$$

where q is the ambient ionization source rate, t is time and α_{eff} is the effective recombination coefficient. We assume that the rate of the ionization q decreases linearly with time during the heating experiment (dotted line in Fig. 6). We use the continuity equation (4) for electrons in this form, assuming that in the E-region and upper D-region the electrons can disappear mainly by reactions of dissociative recombination with positive ions.

The dependence of electron density N_e on electron temperature T_e, is due to the dependence of the recombination coefficient α_{eff}, on T_e (Gurevich and Shvartsburg, 1973):

$$\alpha_{eff}(T_e) = \frac{1}{N_e}\left(5\times10^{-7}\left(\frac{300}{T_e}\right)^{1.2}[NO^+] + 2.2\times10^{-7}\left(\frac{300}{T_e}\right)^{0.7}[O_2^+]\right) \quad (5)$$

Having a disturbed electron temperature value for every 0.5 km, we get the electron density variations in a 0.5 km grid by solving equation (4) numerically. The resulting values were integrated by altitude from 80 km to 95 km to yield the theoretical time variations of electron density, which are shown in Fig. 6 by dashed line.

The electron densities deduced from the backscattered power data show similar large-scale time variations as the modelled electron densities. During the first heating pulses the electron density increases from pulse to pulse, until the decrease of ionization rate becomes dominant, due to the decrease of the solar zenith angle. Thereafter the electron density starts to decrease. In order to more clearly quantify the effect of the artificial ionospheric heating on the electron density, a model calculation of the time variation of electron density without heating is also shown in fig. 6 by dotted line.

5. Conclusions.

In this work we have analysed large scale time variations of electron density derived from EISCAT radar data during ionospheric heating. The short scale time variations (in the time interval of one heating impulse) are less distinctly seen. In Fig. 2 one can see some evidence of time variation in the recorded backscattered power, which is not exactly of the expected form inside a single heating impulse. However, we had data for 7 heating impulses only. The quantitative analysis needs more information and further experiments.

We obtained the following results:

a) A heater induced change of electron density in the upper D-region and lower E-region was detected by the EISCAT UHF incoherent scatter radar. The magnitude of these variations reaches up 13% of background value.

b) The estimated electron density shows similar large scale time variations as the theoretical one. During the first heating pulses the electron density increases from pulse

to pulse, until the decrease of ionization rate due to the decrease of solar illumination becomes dominant, and the electron density starts to decrease.

c) The short scale time variations (during the heating impulse) are seen to have some so far unexplained features, which need a further study.

Acknowledgments: The authors are grateful to Dr W. B. Lyatsky for useful discussions.

References.

1. Gurevich A. V.and A. B. Shvartsburg Nonlinear phenomena in the ionosphere. M., Nauka, 1973.
2. Stubbe P. and Kopka H. Modulation of the Polar Electrojet by powerful HF waves. *Geophysic. Res.*, 1977, **82,** 2319-2325.
3. Itkina M. A. and Krotova Z. N. Low ionosphere parameter variation under the action of a powerful radiation. *Izv. vuzov. Radiofizika,* 1981, **24**, 415-419.
4. Pashin A. B., Belova E. G. and Lyatsky W. B Magnetic pulsation generation by powerful ground based transmitter. *J. Atmos. Terr. Phys.*, 1985, **57**, 245-252.
5. Belova E. G., Pashin A. B. and Lyatsky W.B. Passage of powerful HF radio wave through the lower ionosphere as a function of initial electron density profiles. *J. Atmos. Terr. Phys.* , 1995, **57**, 265-272.
6. Jones T. B., Robinson T. R., Stubbe P. and Kopka H. EISCAT observations of the heated ionosphere. *J. Atmos. Terr. Phys.*, 1986, **48,** 1027–1035.
7. Schlegel K., Rietveld M. and Maul A., A modification event of the auroral E-region as studied with EISCAT and other diagnostics. *Radio Sci.*, 1987, ***22,*** 1063-1072.
8. Mityakov N. A., Grach S. M., and Mityakov S.N. Ionospheric modification by powerful radio wave. 1989, VINITI, Moscow (in Russian).
9. Honary F., Stocker A. J., Robinson T. R.Jones T. B, Wade N. M., Stubbe P. and Kopka H. EISCAT observations of electron temperature oscillations due to the action of high power HF radio waves. *J. Atmos. Terr. Phys.*, 1993, ***55,*** 1433-1448.
10. Tomko A. A., Ferraro A.I. and H.S. Lee D region absorption effects during high-power radio wave heating. *Radio Sci.*, 1980, **15**, 675-682.

Turunen T. GEN-system A new experimental philosophy for EISCAT radars, *J. Atmos. Terr. Phys.*, 1986, **48,** 777-785.

Figure captions.

Fig. 1 Raw electron density, as function of time and altitude, measured by the EISCAT UHF incoherent scatter radar on 27 April 1985 in Tromso, Norway. The data is integrated for one minute in time and for 6 km in altitude. The heating on and off times are also indicated in the plot. Note that the first heating pulse is due to the tuning of the heating transmitters, and not in cycle with the other heating pulses which are starting from 1230 UT. There is a short data gap after 13.00 UT due to a transmitter crowbar.

Fig. 2 Raw electron density as function of time, integrated over the altitude range from 80 km to 95 km., but keeping the original time resolution of the data, which is 10 seconds. The heating on and off times are also indicated in the plot, except for the first heating pulse which was used for tuning up the transmitter (see Fig. 1).

Fig. 3 (top) Initial electron density profiles accepted for calculation. The electron density upper 78 km was derived from backscattered power measured before the heating. Three electron density profiles below 78 km are model profiles.
(bottom) Calculated electron temperature profiles disturbed due to the heating and corresponding to initial electron density profiles plotted in Fig. 3 a). Undisturbed profile is marked by dotted-dashed line.

Fig. 4 Temporal electron density variations due to heating derived from incoherent radar backscattered power, averaged by running over 230 seconds and corresponding the initial electron density profiles from Fig. 3 (top). Heating status is shown by impulses out of scale.

Fig. 5 Temporal (with 10 seconds resolution) electron density variations due to heating integrated from 80 to 95 km and corresponding to initial electron density profile marked in Fig. 3 (top) by dashed line.

Fig. 6 Electron density variations as in Fig. 5 but using 230 seconds running averaging. Solid and dashed lines correspond to derived and simulated electron density, respectively. Dotted line is interpolation of electron density behavior without heating.

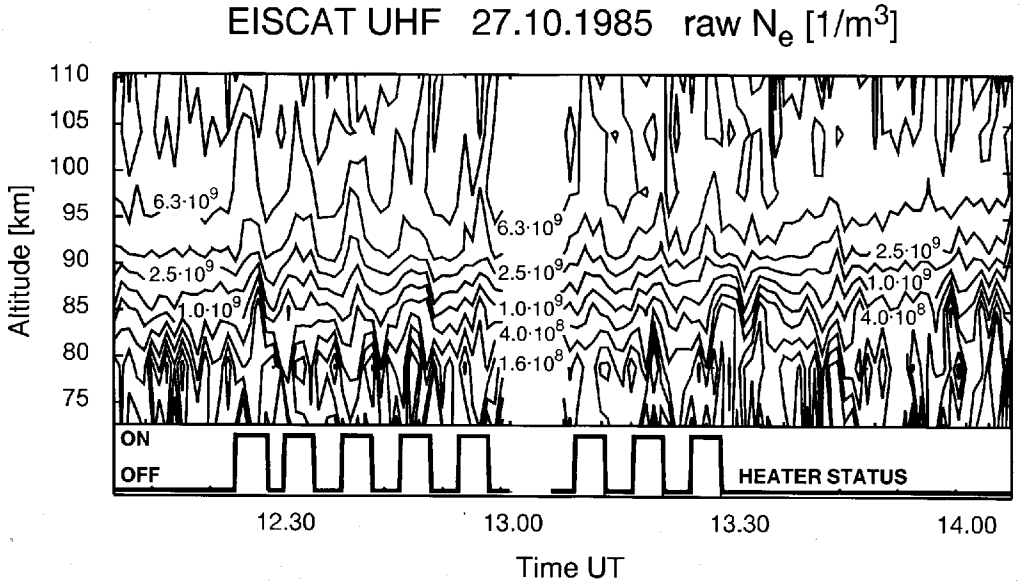
EISCAT UHF 27.10.1985 raw N_e [1/m^3]
Altitude [km]
110
105
100
95
90
85
80
75
6.3·10^9
2.5·10^9
1.0·10^9
6.3·10^9
2.5·10^9
1.0·10^9
4.0·10^8
1.6·10^8
2.5·10^9
1.0·10^9
4.0·10^8
ON
OFF
HEATER STATUS
12.30
13.00
13.30
14.00
Time UT

Fig. 1

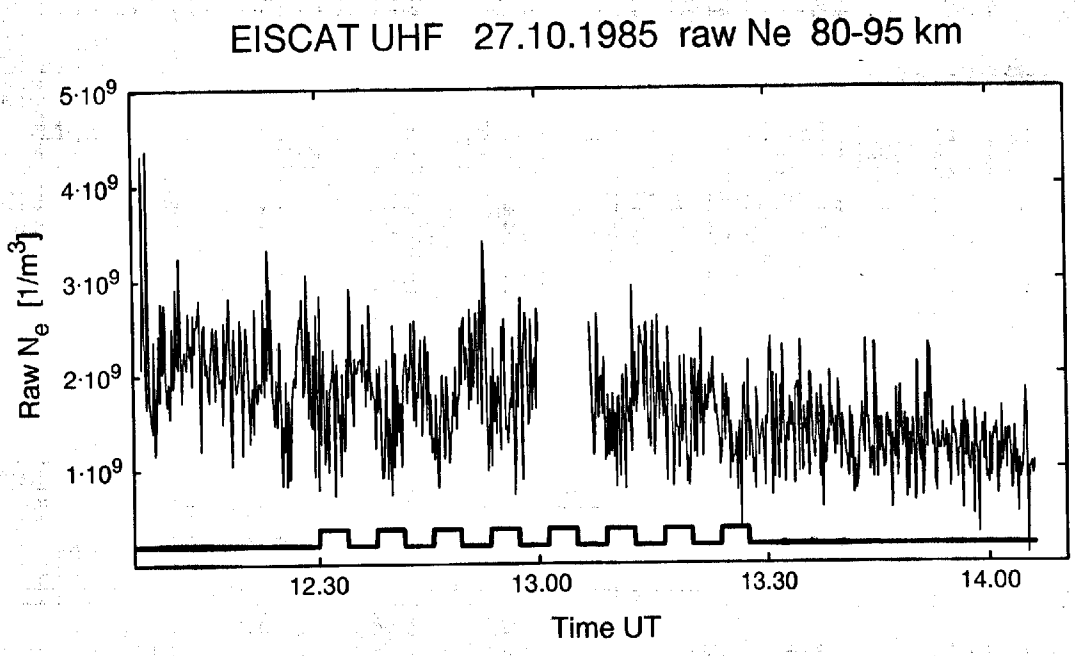
EISCAT UHF 27.10.1985 raw Ne 80-95 km
5·10^9
4·10^9
3·10^9
2·10^9
1·10^9
Raw N_e [1/m^3]
12.30
13.00
13.30
14.00
Time UT

Fig. 2

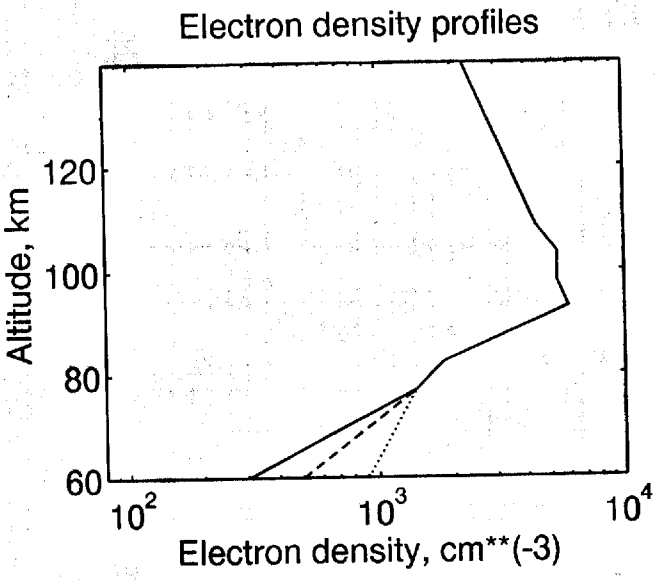
Electron density profiles
Altitude, km
120
100
80
60
10^2
10^3
10^4
Electron density, cm**(-3)

Fig. 3 a)

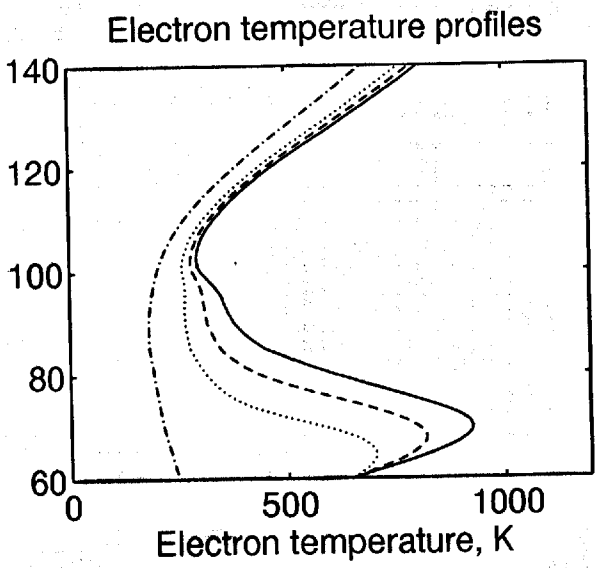
Electron temperature profiles
140
120
100
80
60
0
500
1000
Electron temperature, K

Fig. 3 b)

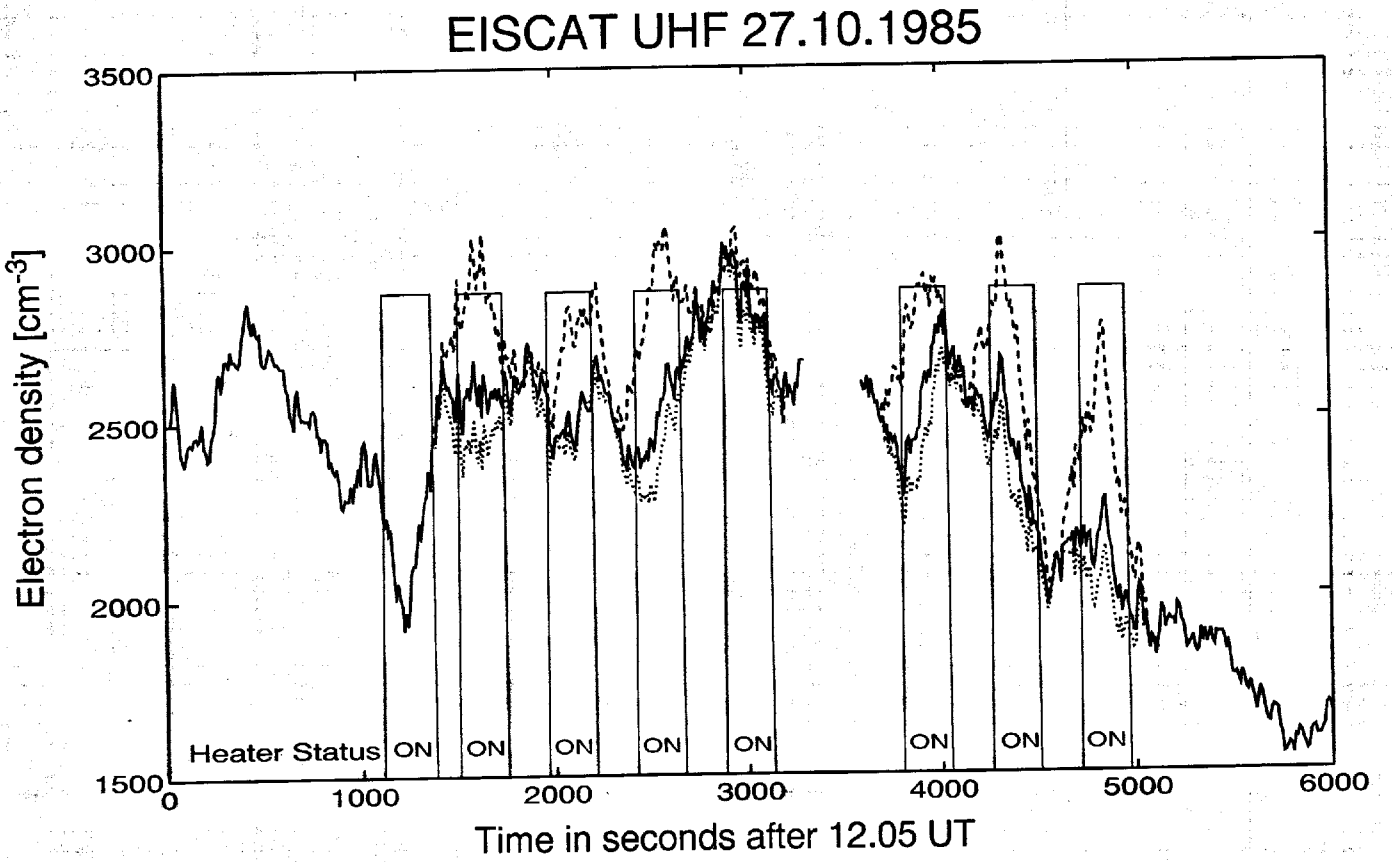
EISCAT UHF 27.10.1985
Electron density [cm-3]
3500
3000
2500
2000
1500
0
1000
2000
3000
4000
5000
6000
Time in seconds after 12.05 UT
Heater Status
ON
ON
ON
ON
ON
ON
ON
ON

Fig. 4

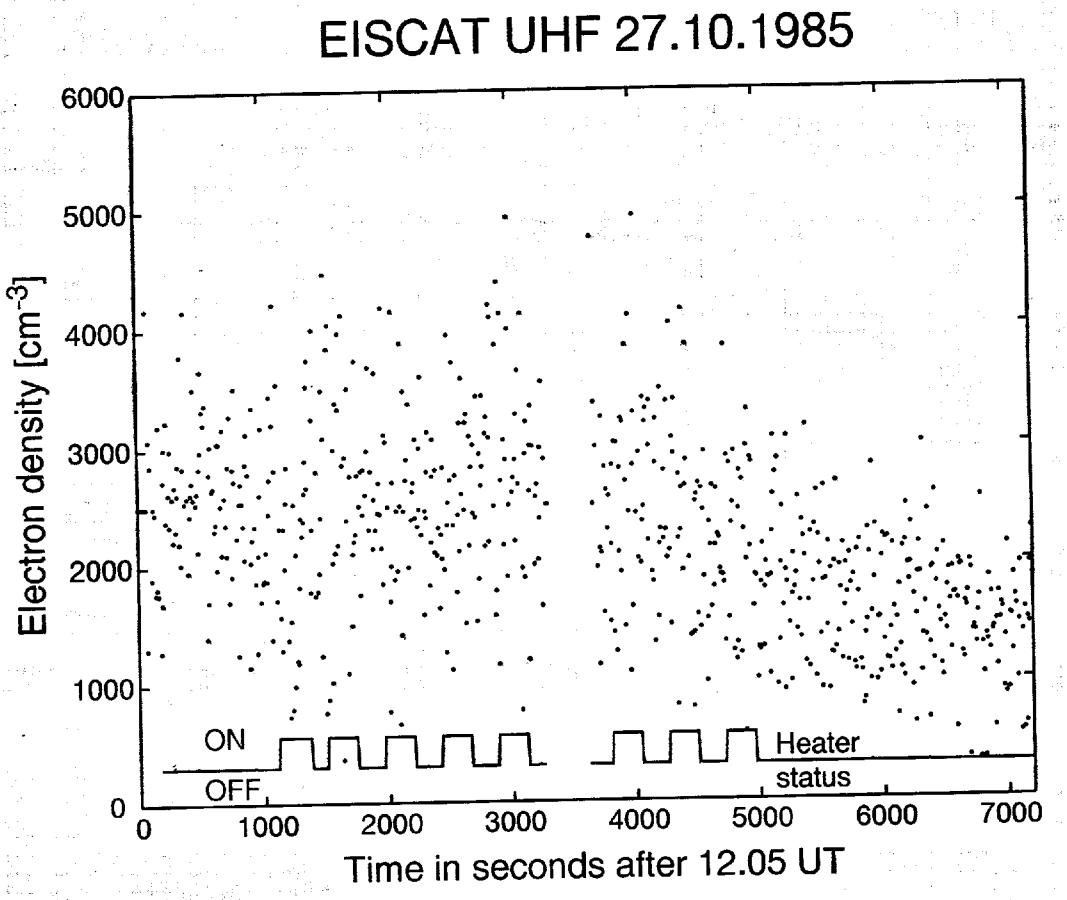
EISCAT UHF 27.10.1985
Electron density [cm-3]
6000
5000
4000
3000
2000
1000
0
ON
OFF
Heater
status
0
1000
2000
3000
4000
5000
6000
7000
Time in seconds after 12.05 UT

Fig. 5

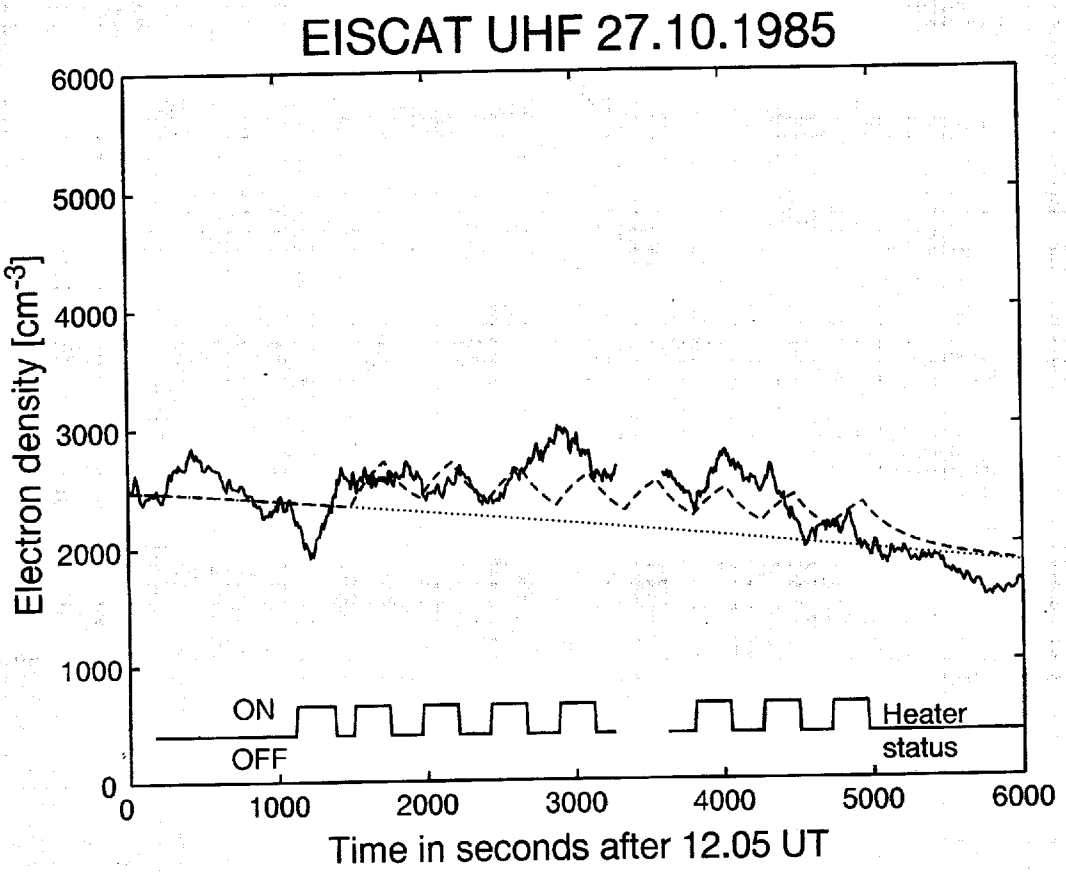
EISCAT UHF 27.10.1985
Electron density [cm-3]
6000
5000
4000
3000
2000
1000
0
0
1000
2000
3000
4000
5000
6000
Time in seconds after 12.05 UT
ON
OFF
Heater
status

Fig. 6